Quantifying the Benefit from Pressure Gradient Data in Wavefield Reconstruction for Time-Lapse Seismic*

Phil Christie[1], Kurt Eggenberger[2], Everhard Muyzert[1], Massimiliano Vassallo[2], and Ali Özbek[1]

Search and Discovery Article #40843 (2011)
Posted November 30, 2011

*Adapted from extended abstract prepared in conjunction with oral presentation at AAPG International Conference and Exhibition, Milan, Italy, October 23-26, 2011

[1]Schlumberger Cambridge Research, Cambridge, UK (pafc1@slb.com)
[2]WesternGeco, London, UK

Abstract

The repeatability of time-lapse seismic data depends critically upon the repeatability of the acquisition geometry. Despite the availability of high precision navigation systems and steerable streamers, matching seismic survey geometries can require spatial over-sampling and/or wavefield interpolation. Because of sparse crossline sampling, this interpolation is usually aliased. Marine streamers exist which acquire acoustic pressure and vertical particle velocity data. It can be shown that the particle velocity vector is intimately related to the pressure gradient vector. If we could acquire the horizontal gradients of the acoustic pressure wavefield in towed marine seismic surveys, this would greatly alleviate the spatial sampling issue by at least doubling the crossline Nyquist wavenumber.

This paper explores the benefit of using inline gradients computed from field data in a simulated crossline reconstruction of seismic wavefields. Finely-sampled pressure and gradient data, from a common sail line acquired in two time-lapse seismic vintages, are taken from a seismic processing flow after surface multiple attenuation. The data are decimated without anti-alias wavenumber filtering and then reconstructed using a variety of algorithms both with and without the gradient measurement. The reconstructed traces are compared with the undecimated data to assess the interpolation errors.

Comparisons are made between the reconstructed traces and the undecimated traces both within the same time-lapse vintage and across the two time-lapse vintages: the former examines only the reconstruction error while the latter estimates the total time-lapse non-repeatability. The errors from reconstructing the data using the gradient information up to twice the pressure-only Nyquist wavenumber are well within acceptable time-lapse bounds and much less than the general survey-to-survey non-repeatability. The use

of a multi-channel interpolation by matching pursuit algorithm, in particular, offers good promise for higher order de-aliasing beyond twice-Nyquist wavenumber.

Introduction

Time-lapse seismic information has proven to be of great value in monitoring offshore reservoirs, where, in contrast to the situation on land, seismic data are good quality and relatively inexpensive while production facilities and wells call for high levels of investment. Suitably planned and executed seismic snapshots can provide field-wide data for input to an integrated reservoir management programme. To be effective, the changes in marine seismic data should signal production-induced changes in the sub-surface and not changes in survey acquisition or data processing. Experience has shown that the repeatability of marine time-lapse seismic data depends upon the repeatability of the acquisition geometry over the spatial variability of the sub-surface geology; non-repeatability of the survey becomes the noise floor for the time-lapse signal from the reservoir (Calvert, 2005; Kragh and Christie, 2002; Misaghi et al., 2007; Næss, 2007). To match two surveys, therefore, we seek to reoccupy corresponding source and receiver positions to an adequate level of accuracy. For small repositioning errors (where small relates in some way to geological variability and seismic wavelength), one would expect the mismatch in the repeated seismic wavefields to be linearly related to the repositioning error and several of the above authors report empirical results which suggest a 'rule of thumb' error gradient of 1% normalised root-mean-square (NRMS) error between two surveys for each 1 m increment in re-positioning error (Kragh and Christie, 2002).

Modern marine seismic surveys accurately report the positions of sources and sensors at shot time. Absolute accuracy is 1-5 m and relative accuracy can reach 10 cm. Vessel positioning – the ability to steer to a pre-defined course – and source positioning controls are also very good. However, depending upon currents, the ability to hold a pre-defined course for the cables can be challenging even for systems with steerable streamers. Consequently, matching source-receiver pairs for different seismic snapshots can require over-sampled acquisition and/or reliance on wavefield interpolation to yield wavefields recorded at corresponding locations between two or more surveys. Over-sampling a survey has direct cost implications and wavefield interpolation, particularly in the coarsely-sampled crossline dimension, can be vulnerable to aliasing problems.

Robertsson et al. (2008) introduced the concept of a multi-component streamer that would measure not only scalar pressure wavefields but also vector wavefields of particle motion such as velocity or acceleration. Because particle motion can easily be converted to a pressure gradient using the vector relation:

$$\nabla P = -\rho \ddot{\mathbf{u}}$$

Where P = acoustic wavefield pressure, ρ = density, and ü = particle acceleration, such a streamer would enable acquisition of both pressure and the 3D gradient of pressure simultaneously. One motivation for recording pressure and the vertical pressure gradient (or acceleration) is to remove the downgoing ghost wavefield, reflected at the sea-surface, by making use of the complementary ghost

responses of the two measurements (Berni, 1984; Robertsson et al., 2004). Combining data from the two sensors extends the usable seismic bandwidth, improving both low frequency deep penetration and high frequency shallow resolution. Such an application has been realised using a two-component seismic streamer measuring pressure and vertical particle velocity (Carlson et al., 2007).

The emerging wavefield is rarely vertical and may have significant components in both the inline and crossline directions. In these situations, a three-component measurement as envisaged by Robertsson et al. (2008) is likely to be beneficial for accurate de-ghosting. Furthermore, signal theory suggests that data from pressure and crossline gradient sensors allow crossline interpolation of the seismic pressure in a spatial bandwidth that is up to twice the Nyquist wavenumber (Linden, 1959). As noted, economic crossline sampling (streamer separation) is sparse compared to inline sampling and is usually aliased. The ability to interpolate time-lapse data onto a common grid with an improved spatial bandwidth could offer significant benefit either in improving the quality of interpolation with current acquisition geometries or possibly in increasing acquisition apertures and hence operational efficiency.

Amundsen et al. (2010) demonstrate that the same theory can be applied to multi-component seabed data. Özbek et al. (2011) show theory for a signal processing approach called Generalised Matching Pursuit (GMP) which can be implemented to realise the extension to the spatial bandwidth offered by the gradient. Vassallo et al. (2010) describe a technique called multi-channel interpolation by matching pursuit (MIMAP) which applies the matching pursuit algorithm to reconstruct the total (up- and down-going) pressure wavefield. MIMAP is the multi-channel extension of interpolation by matching pursuit (IMAP: Özbek et al., 2009; Özdemir et al., 2008) and seeks an optimal set of basis functions which simultaneously minimise the residuals between the modeled and measured pressure and gradient. The samples need not be regular and the pressure and gradient fields need not be sampled at coincident points. MIMAP is data adaptive and, once the basis functions have been determined, the wavefield may be reconstructed at any point, greatly facilitating 4D geometry matching. Because the two measurements impose different constraints on the basis function search, the method has the potential to reconstruct accurately the data even when they are aliased beyond twice the single-component Nyquist wavenumber (Vassallo et al., 2010). Vassallo et al. (2011) showed how pressure and the vertical and crossline gradients of pressure might be used to reconstruct a de-ghosted up-going wavefield at any point within the streamer aperture, even when the input samples are affected by severe aliasing in the crossline direction.

Multi-component data reconstruction has been studied by previous authors using realistic synthetic data. In this paper, we primarily explore the benefit of using real inline gradient data to reconstruct the total pressure wavefield up to twice-Nyquist in a simulated crossline experiment and show that the errors are within normal 4D tolerances.

Method

The Norne Oil Field is located in the Norwegian Sea in 380 m water depth and is producing from Jurassic sandstones at about 2500 m reservoir depth. The field was discovered in 1992 and first oil was in 1997. Reservoir quality is good with porosity ranging from 25-32%. There is a gas cap of about 75 m and an oil column of about 110 m (Osdal et al., 2006). The field has been the target for several vintages of time-lapse seismic surveys, carried out with towed, single-sensor hydrophone streamers beginning in 2001, as part of an integrated reservoir monitoring programme (Goto et al., 2004; Osdal et al., 2006). Data repeatability is considered excellent (Christie et al., 2004). Because no crossline velocity or acceleration data were available, finely-sampled inline pressure data were simply differenced to compute inline gradients which were then resampled to emulate crossline cable separations. The overall workflow is summarised in Figure 1.

The test data comprised 822 shot gathers selected from two matching sail-lines acquired from two Norne survey snapshots in 2004 and 2006. The sail-lines were located towards the edge of the field where there should be no time-lapse reservoir signal. The gathers, sampled at 12.5 m inline trace separation, were taken after surface-related multiple elimination (SRME) out to a maximum source offset of about 1600 m and high-cut filtered to 60 Hz, which is the Nyquist frequency for water-borne arrivals. Inline pressure gradients were computed from two-point differences on the 2006 survey only and interpolated back onto the hydrophone locations. Both pressure and gradient datasets from just the 2006 survey were decimated, without wavenumber filtering, to 25 m (2:1 trace drop) and 50 m (4:1 trace drop: see Fig. 2).

The decimated wavefields from the 2006 vintage were then reconstructed back to 12.5 m sampling using different algorithms, with and without gradients, sorted into CMP gathers and compared, after 2004 vintage. Data from both surveys were stacked using the velocity model from the 2004 survey and repeatability metrics were computed using only data from reconstructed trace locations. Consequently the stacked traces have variable fold, which affects overall trace quality, but the undecimated reference stacks include only traces corresponding to the reconstructed locations so that the comparison is valid. 822 shots were used in the analysis to produce about 20 km of stacked sections which were evaluated with time-windowed 4D metrics. Because of the limited aperture, the reduced fold of the 2D stack, the incomplete demultiple sequence and the lack of migration, the signal-to-noise ratio of these stacks does not approach that of the fully processed Norne datasets but, by carefully matching the processing parameters across comparable datasets, the test analysis offers insights into the performance of the reconstruction algorithms.

Results

Figure 3 shows high signal-to-noise ratio for the computed inline gradient, even at short offsets and late times, when incident wavefields are close to vertical and the gradient signal would be expected to be low. A spectral boost to higher frequencies and

extensive diffraction tails are evident in the gradient gather. The figure demonstrates that the inline component of the gradient forms a measurable, coherent wavefield.

Four interpolators were tested using the workflow in Figure 1. In addition to MIMAP and a generic, single-component sinc interpolator (SINC), NMO-SINC was used whereby reflections were de-aliased with normal moveout (NMO) corrections prior to SINC interpolation. A second gradient algorithm was also used, labeled Y4G, which is essentially a two-component sinc interpolator (Robertsson et al., 2008) that uses both pressure and gradient. Only MIMAP uses generalised matching pursuit.

Figure 4 shows SINC and MIMAP reconstructions of a sample shot gather, decimated to 25 m and 50 m, back to 12.5 m. The undecimated gather (left) is a reference. SINC interpolation shows residual energy, especially at the seabed reflection, at both 2:1 and 4:1 reconstructions. The residuals represent energy aliased up to twice the pressure-only Nyquist frequency for the 25-m decimation and up to four times the pressure-only Nyquist for the 50-m decimation. MIMAP shows very low residual at the seabed for 2:1 reconstruction but has some aliased energy at 4:1 reconstruction.

The reconstructed data were stacked as described above and difference plots between the reconstructed stacks and the corresponding reference stacks were computed for display and repeatability analysis. An example is shown in Figure 5 where the left panel shows the survey non-repeatability between the reference stacks for 2006 and 2004, while the right panel shows the combined residual from the 25-m MIMAP reconstruction error on the 2006 stacks and the survey non-repeatability. Both images are very similar and are dominated by residual multiple and linear diffraction events. Since all gathers were stacked on the primary velocity function, the non-repeating multiples and diffractions leak through the limited demultiple and stack operator. Note that the primary geology, except for the seafloor, is not discernable and neither is the reconstruction error.

Repeatability metrics were computed on the differences between the stacked, reconstructed traces and the corresponding stacked reference traces using 1-s time windows, advanced by 500 ms. Normalised root-mean-square (NRMS) error curves as a function of window time for six interpolation scenarios are shown in Figure 6, which summarises the reconstruction error on single-vintage (2006) data (left) and compares it with the survey errors between the vintages (right).

Discussion

Interpolation error increases with distance and so the errors summarised in Figure 6 represent a worst-case scenario in that they include traces reconstructed at locations mid-way between data points. Even though the gradient noise is that of the pressure from which the gradient is computed and not from a real accelerometer, the simulation is nonetheless representative for the bandwidth,

above the pressure-only Nyquist, over which an accelerometer-derived gradient might be used. We note the following from the left plot in Figure 6:

• BothY4G and MIMAP perform very well on pressure + gradient data below twice-Nyquist on the 25-m data. MIMAP has a slightly higher residual at the seabed than Y4G.

• NMO-SINC performs better than SINC on 25-m decimations to about 3 s TWT, where the data are dominated by strong primary reflections and NMO adequately de-aliases the data. Beyond 3 s, where diffractions and less coherent energy dominate, both SINC and NMOSINC track at levels much worse than the gradient interpolators on the 25-m data.

• The versions of MIMAP and Y4G used in this simulation perform less well on 50-m decimations in the shallow section, at frequencies up to four times pressure-only Nyquist, and Y4G again has a lower seabed residual than MIMAP. The high-amplitude seabed event causes smearing, which can be addressed by an enhanced algorithm.

• Beyond 3 s, MIMAP performs much better than Y4G on diffractions and points to the potential power of MIMAP in higher-order de-aliasing, described in Vassallo et al. (2010) but not fully implemented in this realisation.

From the right plot in Figure 6:

• The green curve shows the survey non-repeatability in the time windows which is dominated by leaked multiple and diffraction energy (Figure 5 left).

• Both MIMAP and Y4G, operating on the 25-m decimations track over the reference curve suggesting that the reconstruction errors and the survey non-repeatability are adding in quadrature and that the reconstruction error is negligible compared to the time-lapse error in this case.

Conclusions

For these versions of MIMAP and Y4G, the gradient reconstruction error for the 25-m decimation is about 7% NRMS at the 2–3-s reservoir level, which is much less than the reported Norne 2003-4 average survey mismatch of 19-21% (Osdal et al., 2006). The reconstruction error is also less than the rule-of-thumb NRMS expected for a positioning error of 12.5 m, and since it appears that reconstruction error will combine in quadrature with other sources of error the analysis presented here suggests that gradient reconstruction would indeed be beneficial in bringing separate time-lapse survey snapshots to a common grid.

Acknowledgements

We thank Statoil, ENI Norge and Petoro for permission to use Norne data in this study. Ian Moore kindly provided the Y4G algorithm. We are also grateful to many Schlumberger colleagues for support and discussions. However, the authors are solely responsible for the material presented here.

References

Amundsen, L., H. Westerdahl, M. Thompson, J.A. Haugen, A. Reitan, M. Landrø, and B. Ursin, 2010, Multicomponent ocean bottom and vertical cable seismic acquisition for wavefield reconstruction: Geophysics, v. 75/6, WB87-WB94.

Berni, A.J., 1984, Marine seismic system: USA Patent 4 437 175.

Calvert, R., 2005, 4D technology: where are we, and where are we going?: Geophysical Prospecting, v. 53, p. 161-171.

Carlson, D., W. Söllner, H. Tabti, E. Brox, and M. Widmaier, 2007, Increased resolution of seismic data from a dual sensor streamer cable: 74th SEG Annual International Meeting, v. 26, p. 994-998.

Christie, P., S. Pickering, and E. Kragh, 2004, Measuring and improving time-lapse seismic repeatability: Offshore Technology Conference, Paper, OTC 16933.

Goto, R., D. Lowden, J.O. Paulsen, B. Osdal, and H.A. Aronsen, 2004, Norne Steered Streamer 4D Case Study: 66th Meeting European Association of Geoscientists and Engineers, Extended Abstract, H021.

Kragh, E., and P. Christie, 2002, Seismic repeatability, normalized RMS, and predictability: The Leading Edge, v. 21/7, p. 640-647.

Linden, D.A., 1959, A discussion of sampling theorems: Proceedings of the Institute of Radio Engineers, v. 47, p. 1219-1226.

Misaghi, A., M. Landrø, and S.A. Petersen, 2007, Overburden complexity and repeatability of seismic data: Impacts of positioning errors at the Oseberg Field, North Sea: Geophysical Prospecting, v. 55, p. 365-379.

Næss, O., 2007, The Relationship between Geometrical Repeatability and Seismic Trace Repeatability in 4D: 69th Meeting European Association of Geoscientists and Engineers, Extended Abstract, PO66.

Osdal, B., O. Husby, H.A. Aronsen, N. Chen, and T. Alsos, 2006, Mapping the fluid front and pressure buildup using 4D data on Norne Field: The Leading Edge, v. 25, p. 1134-1141.

Özbek, A., K. Özdemir, and M. Vassallo, 2009, Interpolation by matching pursuit: 79th SEG Annual International Meeting, p. 3254-3257.

Özbek, A., M. Vassallo, K. Özdemir, D.-J. van Manen, K. Eggenberger, and J.O.A. Robertsson, 2011, Parametric matching pursuit methods to reconstruct seismic data acquired with multichannel sampling: 73rd Meeting European Association of Geoscientists and Engineers, Extended Abstract, A042.

Özdemir, K., A. Özbek, and M. Vassallo, 2008, Interpolation of Irregularly Sampled Data by Matching Pursuit: 70th Meeting European Association of Geoscientists and Engineers, Extended Abstract, G025.

Robertsson, J.O.A., and E. Kragh, 2004, Method and system for reducing effects of sea surface ghost contamination in seismic data: USA Patent 6 775 618.

Robertsson, J.O.A., I. Moore, M. Vassallo, K. Özdemir, D.-J. van Manen, and A. Özbek, 2008, On the use of multicomponent streamer recordings for reconstruction of pressure wavefields in the crossline direction: Geophysics, v. 73/5, A45-A49.

Vassallo, M., A. Özbek, K. Eggenberger, K. Özdemir, D.-J. van Manen, and J.O.A. Robertsson, 2011, Matching pursuit methods applied to multicomponent marine seismic acquisition – the issue of crossline aliasing: 73rd Meeting European Association of Geoscientists and Engineers, Extended Abstract, A043.

Vassallo, M., A. Özbek, K. Özdemir, and K. Eggenberger, 2010, Crossline wavefield reconstruction from multicomponent streamer data, Part 1: Interpolation by matching pursuit using pressure and its crossline gradient: Geophysics, v. 75, WB53-WB67.

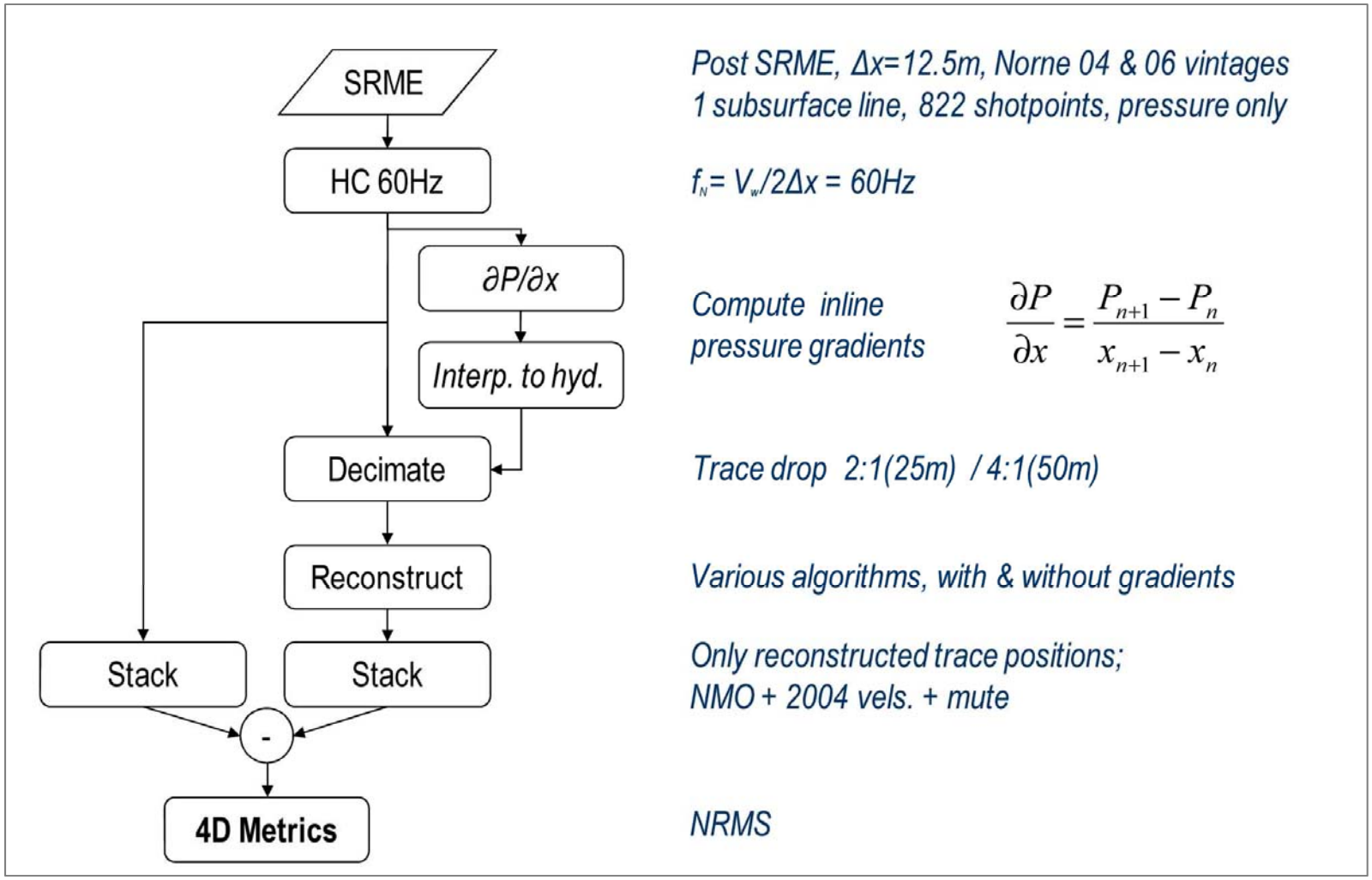

Figure 1. Workflow for computing repeatability metrics from reconstructed data in comparison with undecimated data and across vintages.

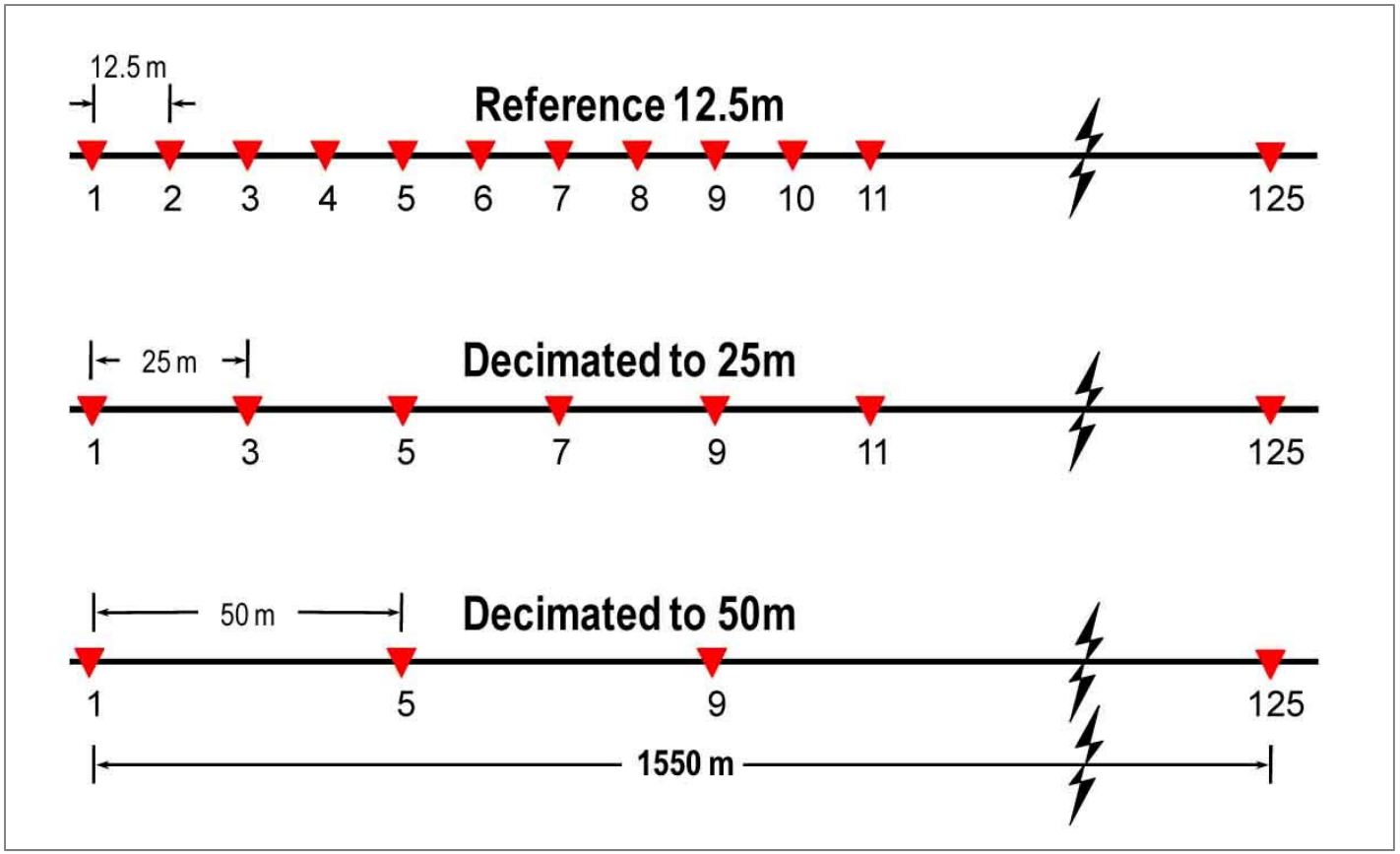

Figure 2. Schematic diagram of the inline sampling along the seismic cable which provides the trace spacing of the reference shot gathers for both 2004 and 2006 (top), and the 2006 gathers decimated to 25 m (middle), and 50 m (bottom) for input into trace reconstruction. After sorting to common mid-point, only reconstructed traces were stacked, using the 2004 velocity function, so that final stack fold depends on the decimation. Reference stacks comprise corresponding traces.

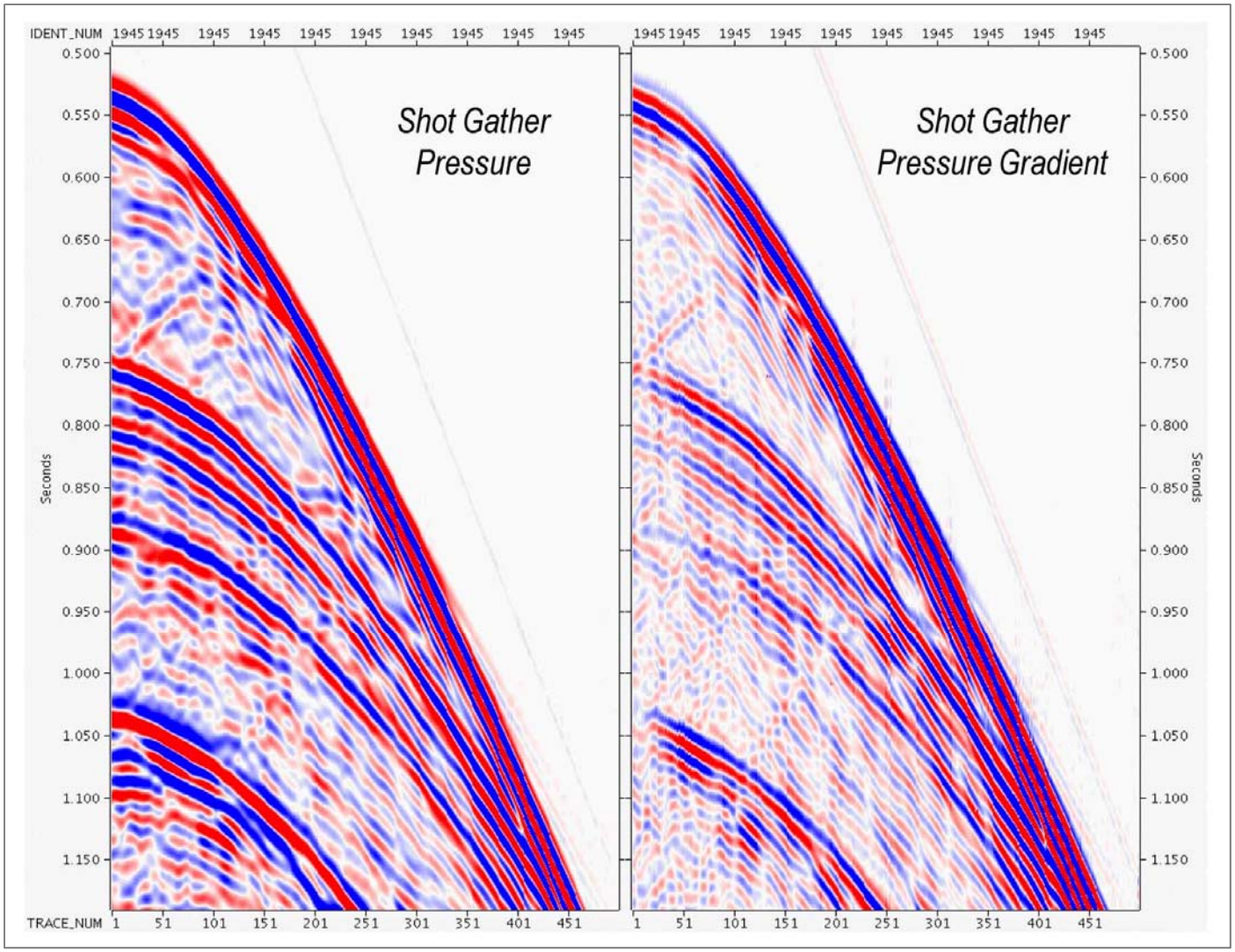

Figure 3. Sample inline shot gathers for pressure (left) and computed pressure gradient (right). The data, sampled at 12.5 m, were then decimated to 25 m and 50 m. Gradient scaled up by 12.5.

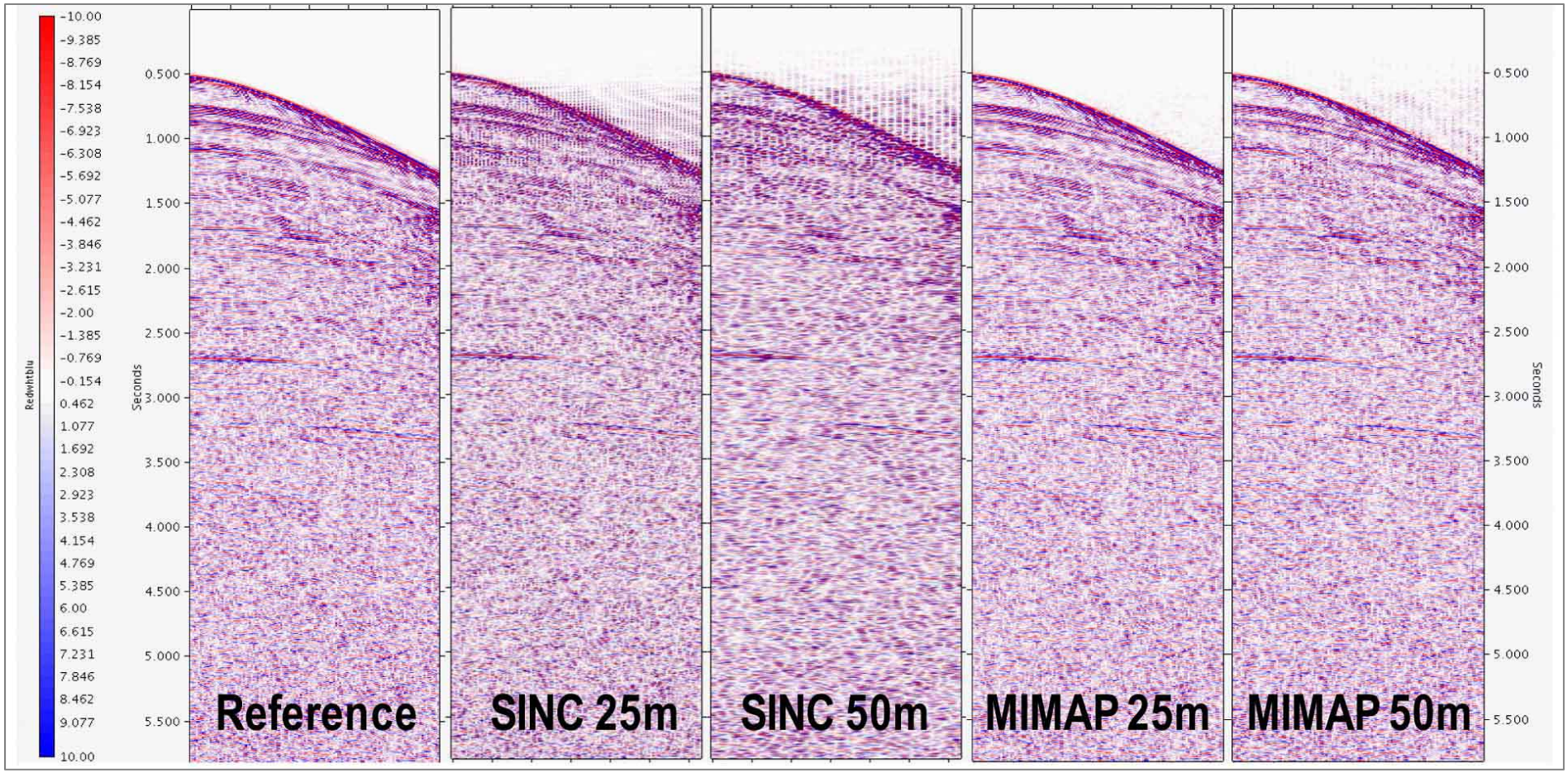

Figure 4. Sample gather reconstructions from 25-m and 50-m decimations using pressure-only (SINC) and pressure + gradient (MIMAP). The undecimated gather is shown, left, for reference.

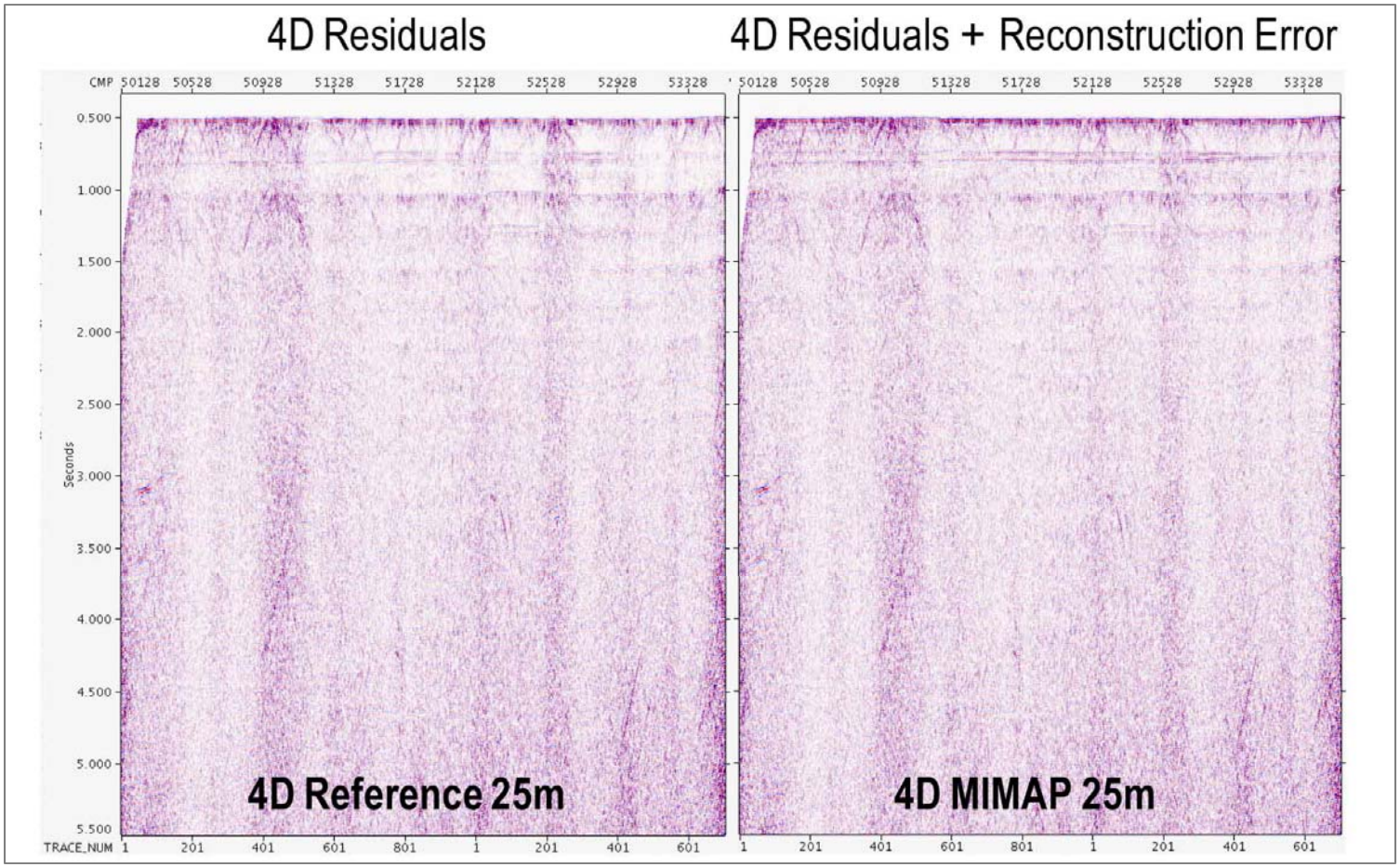

Figure 5. (left) Difference plots between 2006 and 2004 reference stacks, and (right) the 25-m MIMAP reconstructed 2006 stacks and 2004 reference stacks. Neither primary geology nor reconstruction error is evident in the display.

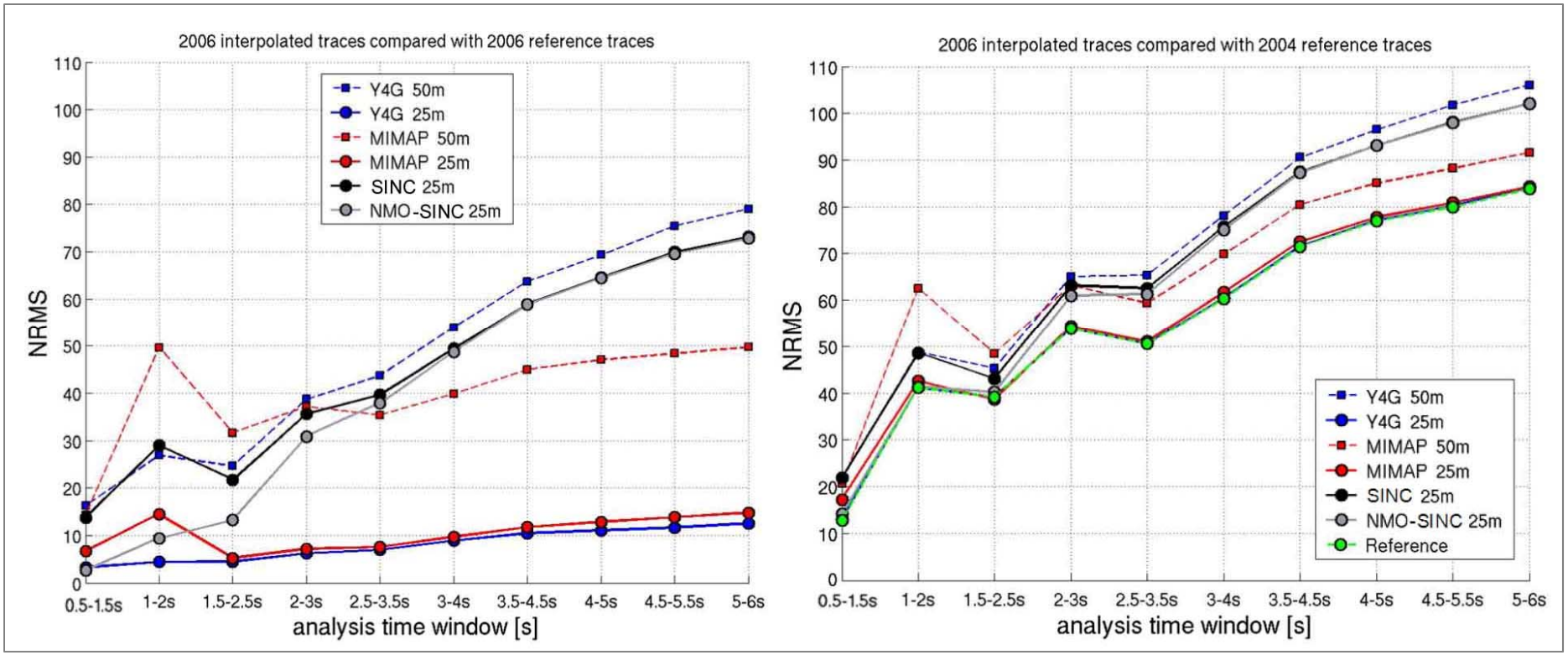

Figure 6. (left) NRMS between reconstructed and undecimated 2006-vintage traces computed in 1000 ms windows for six interpolations. (right) NRMS between the 2006 reconstructed data and the 2004 reference data. The left plot displays only reconstruction error while the right plot shows combined residuals from survey non-repeatability and reconstruction error. Note the survey non-repeatability from the green curve on the right. See text for further detail and discussion.